Title:

Cytosolic Sensor of Bacterial Lipopolysaccharide in Human Macrophages

Authors:

Maricarmen Rojas-Lopez[1†], Amanda S. Zajac[1†], Thomas E. Wood[1†], Kelly A. Miller[1†], María Luisa Gil-Marqués[1], Austin C. Hachey[1], Vritti Kharbanda[1], Keith T. Egger[1], Marcia B. Goldberg[1,2,3,4*]

Affiliations:

[1]Center for Bacterial Pathogenesis, Division of Infectious Diseases, Department of Medicine, Massachusetts General Hospital and Harvard Medical School, Boston, MA, USA.

[2]Department of Microbiology, Blavatnik Institute, Harvard Medical School, Boston, MA, USA.

[3]Broad Institute of MIT and Harvard, Cambridge, MA, USA.

[4]Department of Immunology and Infectious Diseases, Harvard T.H. Chan School of Public Health, Boston, MA, USA.

[†]These authors contributed equally to this work.

*Correspondence should be addressed to M.B.G. (marcia.goldberg@mgh.harvard.edu), ORCID number: 0000-0003-4266-9733

Summary paragraph

Inflammasomes are cytosolic supramolecular organizing centers that, in response to pathogen-derived molecules and endogenous danger signals, assemble and activate innate immune responses[1-4]. Bacterial lipopolysaccharide (LPS) is an inflammasome trigger and a major mediator of inflammation during infection. Activation of most inflammasomes is triggered by sensing of pathogen products by a specific host cytosolic NLRP or other sensor protein that then activates a pro-inflammatory caspase. LPS that accesses the cell cytosol (cLPS) induces cell-autonomous activation of a non-canonical inflammasome that contains caspases-4/5 in humans or caspase-11 in mice[5-7]. Whereas the NLRPs that sense most pathogen triggers have been identified, no NLRP is known to sense cLPS, which together with the observation that caspases-4, -5, and -11 bind LPS *in vitro*[8], has led to the postulate that inflammasome activation by cLPS occurs independent of an NLRP. Here we show that in response to infection by gram-negative intracellular bacterial pathogens or to LPS transfection, efficient activation of the non-canonical pathway in human-derived macrophages depends on primate-specific NLRP11. Further, in both immortalized human-derived macrophages and primary human macrophages, NLRP11-dependent cell death is specifically due to detection of cLPS. In cell lysates, NLRP11 binds LPS independently of caspase-4 and caspase-4 independently of LPS. Our results demonstrate that NLRP11 senses cLPS and promotes LPS-dependent activation of caspase-4. NLRP11 is a previously missing link and a component of the human non-canonical inflammasome activation pathway.

Introduction

Inflammasomes assemble in response to the presence in the cytosol of pathogen-associated molecules, including dsDNA, flagellin, type 3 secretion system structural proteins, pore-forming toxins, ion flux, ATP, and LPS[1-4]. Canonical inflammasomes consist of a sensor protein and an inflammatory caspase, frequently linked by an adaptor protein. Inflammasome assembly activates inflammatory caspases, which proteolytically process the pore-forming protein gasdermin D[9-12]. In the caspase-1 inflammasome, caspase-1 proteolytically processes the pro-inflammatory cytokines IL-18 and IL-1β[13,14], which are released through pores formed in the plasma membrane by the N-terminal domain of gasdermin D; these pores are required both for the release of activated pro-inflammatory cytokines and for pyroptotic cell death[9-12,15]. The presence of bacterial LPS in the cytosol of human macrophages activates a non-canonical inflammasome, which in humans, contains caspases-4 and -5, and in mice, caspase-11[5-7], and which also leads to caspase-mediated processing of gasdermin D, pore formation, and pyroptotic cell death. To date, no sensor protein of cytosolic LPS has been identified, and because caspase-4, -5, and -11 bind LPS *in vitro*[8], the current paradigm is that the non-canonical inflammasome lacks a sensor protein (Fig. 1a).

NLRP11 required for cell death due to intracellular gram-negative pathogens

In a forward genetic screen that enriched for genes required for death during infection with the gram-negative intracellular bacterial pathogen *Shigella flexneri*, we identified the primate-specific protein NLRP11[16] (Extended Data Fig. 1); the screen was conducted using a human-derived myeloid lineage cell line. The NLRP (nucleotide-

62 binding oligomerization domain, leucine rich repeat and pyrin domain containing protein)
63 family includes proteins such as NLRP1 and NLRP3 that sense a range of pathogen-
64 associated molecular patterns or damage-associated molecular patterns in the cell
65 cytosol. We performed targeted deletion of *nlrp11* in the human-derived monocyte cell
66 line THP-1 and found that cell death during *S. flexneri* infection (as measured by lactate
67 dehydrogenase (LDH) release) was significantly reduced for macrophage-like cells that
68 lack NLRP11. In each of two THP-1-derived cell lines in which *nlrp11* was disrupted by
69 a CRISPR-Cas9 induced indel (Extended Data Fig. 2), release of LDH upon infection
70 with *S. flexneri* was reduced by more than 50% (Fig. 1b). Consistent with previous
71 reports, *S. flexneri*-induced macrophage cell death was dependent on the bacterial type
72 3 secretion system, which mediates both bacterial uptake[17] and vacuolar escape[18,19], as
73 a mutant that lacked either the virulence plasmid that encodes this secretion system or
74 *virB*, the transcriptional activator of this system, displayed minimal cell death (Extended
75 Data Fig. 3a).

76 To test whether the dependence on NLRP11 for efficient cell death was generalizable to
77 other intracellular gram-negative bacterial pathogens, we infected *NLRP11*$^{-/-}$ cells with
78 the cytosolic pathogen *Burkholderia thailandensis* and the intracellular but largely
79 vacuolar pathogen *Salmonella enterica* serovar Typhimurium. As with *S. flexneri*
80 infection, in the absence of NLRP11, cell death during infection with *B. thailandensis* or
81 *S.* Typhimurium was significantly reduced (Fig. 1c-d). In response to viral infection and
82 certain Toll-like receptor interactions, the NF-κB pathway is repressed by NLRP11-
83 dependent targeted degradation of TRAF6[20-22]; however, *S. flexneri*-induced NLRP11-
84 dependent cell death was independent of TRAF6, whether or not the *Shigella* effector

85 OspI, which suppresses TRAF6 signaling[23], was present (Extended Data Fig. 3b-d),
86 indicating that the role of NLRP11 in bacterial infection-induced cell death is distinct
87 from its role in NF-κB signaling. Together, these results indicate that NLRP11 is
88 required for efficient cell death induced by multiple intracellular gram-negative
89 pathogens and raised the possibility that the implicated pathogen-associated trigger of
90 cell death is generally present among gram-negative bacteria and depends on
91 intracellular presentation.

92 **NLRP11 recognizes cLPS**

93 We tested whether LPS, which is specific to the cell envelope of gram-negative
94 bacteria, might be required for NLRP11-dependent cell death. Infection of THP-1
95 macrophages with the cytosolic gram-positive pathogen *Listeria monocytogenes*
96 induced minimal levels of cell death during the timeframe of the experiment, but when
97 coated with *S. enterica* LPS, induced cell death that was largely dependent on NLRP11
98 (Fig. 2a). The observed cell death was dependent on cytosolic localization, as a *L.*
99 *monocytogenes* strain lacking listeriolysin O (LLO), which is required to lyse the
100 vacuole[24], induced minimal cell death. Introduction of LPS alone directly into the cytosol
101 by electroporation similarly induced cell death that was significantly dependent on
102 NLRP11, both in *NLRP11*$^{-/-}$ and NLRP11 siRNA-treated THP-1 macrophages (Fig. 2b-
103 c), whereas cell death induced by extracellular LPS was independent of NLRP11
104 (Extended Data Fig. 4a). These data indicate that NLRP11 functions in a cell death
105 pathway that is activated by LPS localized to the cytosol (cLPS). For pathogens such as
106 *Salmonella* that do not themselves efficiently lyse the vacuole, delivery of LPS to the

107 cytosol occurs upon guanylate-binding protein (GBP) 2-mediated vacuolar lysis[25], a
108 potential explanation for the lack of differential NLRP11-dependent cell death induced
109 by wild-type *S.* Typhimurium, which is largely vacuolar, and *sifA* mutant *S.*
110 Typhimurium, which is predominantly cytosolic[26] (Fig. 1d).

111 **NLRP11 required for efficient activation of non-canonical inflammasome**

112 We tested whether NLRP11 was required for activation of the non-canonical
113 inflammasome, which in humans, contains caspases-4 and -5. Activation of caspase-4
114 and the downstream pore-forming protein gasdermin D were dependent on NLRP11;
115 during *S. flexneri* infection, processing of caspase-4 and gasdermin D, leading to the
116 release of active domains of each, was significantly reduced in the absence of NLRP11
117 (Fig. 1e-f). In THP-1 macrophages depleted of caspase-4, the absence of NLRP11
118 caused no significant additional decrease in cell death induced by LPS transfection (Fig.
119 2d and Extended Data Fig. 5a). Depletion of *CASP1* or *MyD88* was associated with no
120 significant decrease in cell death in response to cLPS as compared to control depletion
121 for either THP-1 macrophages containing NLRP11 or THP-1 macrophages lacking
122 NLRP11 (Fig. 2d and Extended Data Fig. 5b). Despite testing several antibodies, we
123 were unable to detect native cellular NLRP11 by western blot, presumably due to very
124 low levels of native protein. These data indicate that NLRP11 is required for efficient
125 activation of the non-canonical inflammasome, likely functioning in the caspase-4
126 pathway, and that NLRP11 function is independent of caspase-1 and extracellular Toll-
127 like receptor signaling. Consistent with NLRP11 functioning specifically in the non-
128 canonical inflammasome pathway, NLRP11 was not required for activation of the

129 canonical NLRP3 inflammasome, as cell death induced by the NLRP3 agonist nigericin
130 was independent of NLRP11 (Extended Data Fig. 4b-d).

131 **NLRP11 interacts with LPS and caspase-4**

132 In contrast to NLRP3 and NLR family CARD domain containing 4 (NLRC4)
133 inflammasomes, activation of the non-canonical pathway is independent of the adaptor
134 protein ASC, as signaling in response to cytosolic LPS is normal in human or mouse-
135 derived macrophages lacking ASC[6,8] and NLRP11 does not co-localize with ASC
136 specks[20,27]. We tested whether NLRP11 interacts with other core components of the
137 non-canonical pathway by ectopic expression of selected components in HEK293T
138 cells, which lack most innate immune proteins, including ASC and inflammatory
139 caspases. Biotin-conjugated LPS precipitated NLRP11 in the absence of caspase-4
140 (Fig. 3a), indicating that NLRP11 binds LPS independently of caspase-4. As previously
141 described[8], LPS also specifically precipitated caspase-4 and its catalytically inactive
142 derivative (CASP4 C258A), including in the presence of NLRP11 (Fig. 3b), whereas the
143 triacylated lipid Pam3CSK4 did not precipitate either NLRP11 or, as previously
144 described[8], caspase-4 (Fig. 3a). In addition to binding to LPS independent of caspase-
145 4, NLRP11 specifically precipitated caspase-4 (Fig. 3c). To characterize the binding
146 relationship of NLRP11 to caspase-4, we developed a plate binding assay using FLAG-
147 NLRP11 in HEK293T cell lysates and purified caspase-4 (Methods and Extended Data
148 Fig. 6a). In this assay, FLAG-NLRP11 binding depended on caspase-4, as binding of
149 FLAG-NLRP11 in the absence of caspase-4 was at background levels (Fig. 3d,
150 diamonds). Moreover, binding of NLRP11 to caspase-4 increased as a function of

151 increasing concentrations of both NLRP11 lysate and caspase-4, resembling the
152 asymptotic phase of a sigmoidal curve, beginning to reach saturation at 8-10 μg/ml
153 caspase-4 coating the wells (Fig. 3d).

154 **NLRP11 displays caspase specificity**

155 In addition to caspase-4, NLRP11 co-precipitated with caspase-1; of note, NLRP11 did
156 not co-precipitate with caspase-5, a paralog of caspase-4 that binds LPS and is a
157 component of at least some non-canonical inflammasomes[8,14,28], or the more divergent
158 caspase-9 (Fig. 3e and Extended Data Fig. 7a). In these experiments the isoform of
159 caspase-5 that was used was caspase-5/a, the most abundant isoform; although this
160 isoform contains nearly all sequences present in other isoforms, it is theoretically
161 plausible that another isoform(s) would interact with NLRP11. Although caspase-1 co-
162 precipitates with NLRP11 (Fig. 3e), NLRP11 does not activate caspase-1 under
163 conditions in which AIM2 did [20], and NLRP11 function in LPS-induced cell death of
164 THP-1 macrophages is independent of caspase-1 (Fig. 2d), indicating that the observed
165 interaction of caspase-1 with NLRP11 contributes minimally to activation of the non-
166 canonical inflammasome.

167 **NLRP11 role in non-canonical inflammasome activation is independent of**
168 **interferon-gamma and guanylate-binding protein-1**

169 Host GBPs bind intracellular LPS, promote non-canonical inflammasome activation[29-33],
170 and are encoded by genes that are strongly induced by interferon-gamma (IFNγ)[34].
171 Human GBP1 binds LPS on the *S. flexneri* surface, whereupon it enhances caspase-4

172 recruitment[35]. We tested whether IFNγ stimulation altered the role of NLRP11 in
173 activation of the non-canonical inflammasome. IFNγ pre-treatment of THP-1
174 macrophages induced GBP1, as expected, yet NLRP11 was still required for efficient
175 activation of *S. flexneri*-induced cell death (Extended Data Fig. 8a-b). Moreover, during
176 the timeframe of this infection, GBP1 was not induced by *S. flexneri* infection alone,
177 depending exclusively on pre-treatment with IFNγ (Extended Data Fig. 8c), indicating
178 that is not required for non-canonical inflammasome induced pyroptosis or NLRP11
179 function in non-canonical inflammasome induced pyroptosis. Moreover, IFNγ and GBP1
180 do not bypass the requirement for NLRP11 in this pathway.

181 **Requirement for NLRP11 in primary human macrophages**

182 Following treatment of primary human monocyte-derived macrophages with siRNA to
183 NLRP11, although overall levels of cell death are lower than for immortalized THP-1
184 cells, cell death induced by cLPS was significantly diminished (Fig. 2e). As in THP-1
185 macrophages, in primary macrophages, the defect in cLPS-induced cell death
186 depended on caspase-4, but not MyD88 (Figs. 2f-g and Extended Data Fig. 5c-d),
187 indicating that in these assays, the trigger was cLPS rather than extracellular LPS, and
188 demonstrating that the requirement for NLRP11 in the non-canonical inflammasome
189 pathway extends to primary human cells.

190 In summary, the data reported here identify NLRP11 as a primate-specific cytosolic
191 sensor of bacterial LPS in the activation of the caspase-4 dependent inflammasome and
192 caspase-4 dependent pyroptosis. These functions imply that NLRP11 is a key
193 component of this inflammasome. Galectin-3, one among a family of β-galactoside–

194 binding proteins, senses cytosolic pathogens, promotes delivery of GBPs to ruptured
195 pathogen-containing vacuoles, and enhances assembly of LPS-triggered caspase-4/11
196 oligomerization and activation[36-38]. Whether galectin-3 activity synergizes with the
197 interaction of cLPS and NLRP11 is uncertain; however, the independence of NLRP11
198 function from GBP1 (Extended Data Fig. 8) suggests that any contribution of galectin-3
199 to this process would be minor. Additionally, it remains uncertain whether the unique
200 presence of NLRP11 in primates and the absence of it or identifiable homologs in mice
201 contributes to the observed ~10^4-fold increased susceptibility to gram-negative bacterial
202 sepsis and LPS of humans as compared to mice[39,40]; additional insights into these
203 relationships would potentially enable much-needed improved mouse models for the
204 study of bacterial sepsis.

205 **Methods**

206 **Bacterial strains, plasmids, antibodies, and reagents.** *Shigella flexneri* serotype 2a
207 wildtype strain 2457T and the *S. flexneri* mutant strains *virB*::Tn5, BS103, and Δ*ospC3*,
208 which are isogenic to 2457T, have been described previously[41-44]. *Salmonella enterica*
209 serovar Typhimurium and the isogenic Δ*sifA* mutant[26] were gifts from L. Knodler.
210 *Burkholderia thailandensis*[45] was a gift from P. Cotter. *Listeria monocytogenes* 10403s
211 and 10403 LLO^{-}[46] were gifts from M. Kielian and J. Miller. *S. flexneri* was grown
212 overnight in tryptic soy broth at 37°C with aeration. *L. monocytogenes* was grown
213 overnight in brain heart infusion broth at 30°C at a stationary slant. *B. thailandensis* was
214 grown overnight in low salt Luria broth (LB) at 37°C with aeration. *S. enterica*
215 Typhimurium was grown in LB broth at 37°C with aeration.

216 Caspase-1 (Abcam, ab207802) rabbit monoclonal antibody was used at 0.5 μg/mL
217 (1:1000). Caspase-4 (Santa Cruz, sc-56056), and gasdermin D (Santa Cruz, sc-81868)
218 mouse monoclonal antibodies were used at 0.5 μg/mL (1:200). FLAG M2 mouse
219 monoclonal antibody (Sigma, F3165) was used at 76 ng/mL (1:5000). Myc rabbit
220 monoclonal antibody (Cell Signaling, 2278) was used at 1:1000. GBP1 mouse
221 monoclonal antibody (Abcam, ab119236) was used at 1:1000. For western blots of
222 immunoprecipitations, the secondary antibody used was TrueBlot horseradish
223 peroxidase-conjugated anti-mouse Ig (Rockland, 18-8817-31). For detecting β-actin,
224 horseradish peroxidase-conjugated anti-β-actin antibody (Sigma, A3854) was used. For
225 all other western blots, the secondary antibody used was horseradish peroxidase-
226 conjugated goat anti-rabbit or goat anti-mouse IgG antibodies (Jackson

227 ImmunoResearch, 115-035-003 or 111-035-144). All antibodies were diluted in 5% milk
228 in TBST (0.1% Tween).

229 **Strain and plasmid construction.** The *S. flexneri ospI* deletion mutant was generated
230 in the 2457T strain background using the lambda red method by introducing a
231 chloramphenicol acetyltransferase (*cat*) cassette into the *orf169b* gene (which encodes
232 OspI), as described[47].

233 pCMV-CASP4-MYC and pCMV-CASP5-MYC were made from pCMV-CASP4-MYC-
234 FLAG and pCMV-CASP5-MYC-FLAG, gifts from S. Shin. pCMV-CASP4-MYC C258A
235 and pCMV-CASP4-MYC K19E C258A was generated by splicing by overlap extension
236 PCR (SOE-PCR). pcDNA-NLRP11 (gift from H. Wu) was subcloned into pCMV-FLAG
237 with an N-terminal FLAG tag for FLAG-NLRP11 and an N-terminal MYC tag for MYC-
238 NLRP11. All FLAG tags are 3xFLAG. All N-terminal Myc tags are 6xMyc; all C-terminal
239 Myc tags are 1xMyc. All DNA used for transfection was prepared LPS-free (Macherey-
240 Nagel, 740410.50).

241 **Generation of CRISPR knockouts.** THP-1 cells were transduced with lentivirus
242 packaged with pLentiCas9-Blast (Addgene, 52962) generated from HEK293T cells.
243 THP-1 cell suspensions were treated with 8 μg/mL polybrene, combined with lentivirus
244 and centrifuged in 12-well plates for 2 h at 1000 x g at 30°C. After centrifugation, cells
245 were incubated for 2 h and washed once with fresh media. After 48 h, blasticidin
246 (10 μg/mL) was added to the transduced cells. Guide RNA sequence ("sgRNA3",
247 AGGCATGCAAAGCTGTCATG) was subcloned into pLentiGuide-Puro (Addgene,
248 59702). Guide RNA expressing plasmids were packaged into lentivirus using HEK293T

249 cells. Polybrene treated THP-1 cells were transduced and selected with 1 μg/mL
250 puromycin. Cells were limiting diluted and single cell clones were screened by
251 SURVEYOR (IDT, 706020) and Sanger sequencing coupled with TIDE analysis
252 (Brinkman et. al 2014).

253 **Generation of *TRAF6* depletion cell lines.** pLKO.1-shTRAF6 ([48], gift of A. Goldfeld),
254 which encodes shRNA to *TRAF6*, was packaged into lentivirus in HEK293T cells.
255 Lentivirus were introduced into NLRP11+/+ and NLRP11-/- THP-1 cell lines and cells
256 containing pLKO.1-shTRAF6 were selected, expanded by maintenance in 0.8 μg/mL
257 puromycin, as described[48], and stable clones were isolated by limiting dilution.

258 **Mammalian cell culture.** All cell lines were obtained from ATCC. HEK293T cells were
259 maintained in Dulbecco's Modified Eagle's medium (Gibco, 11965118). THP1 cells were
260 maintained in RPMI-1640 (Gibco, 21870092). All media was supplemented with 10%
261 (vol/vol) fetal bovine serum (heat inactivated, sterile filtered, R&D Systems). For THP-1
262 cells, RPMI-1640 media was also supplemented with 10 mM HEPES (Gibco,15630080)
263 and 2 mM L-glutamine (Gibco, 25030081). All cells were grown at 37°C in 5% CO_2. To
264 differentiate monocyte cell lines into macrophage-like cells, 50 ng/mL phorbol-12-
265 myristrate-13-acetate (PMA) was added 48 h before experiments. Where indicated,
266 cells were pretreated with 10 ng/mL IFNγ 16-20 h prior to infection.

267 **Precipitation experiments.** HEK293T cells were transiently transfected using Fugene6
268 (Promega). A stock solution of 10x Buffer A (100 mM HEPES, 1500 mM NaCl, 10 mM
269 EGTA, 1 mM $MgCl_2$, pH 7.4) was prepared. The cell culture medium was removed 24-
270 48 h after transfection. Cells were washed with cold PBS and lysed in 1x Buffer A, 0.5%

271 Triton-X. Cell lysates were incubated on ice for 15 min, vortexed for 15 s and
272 centrifuged at 13,200 rpm for 10 min at 4°C. The pellet was discarded, and Bradford
273 assay was used to determine protein concentration. 30 μL of FLAG M2 Magnetic Beads
274 (Millipore-Sigma, M8823) were washed twice in 1x Buffer A, 0.1% Triton-X and
275 equilibrated in the same buffer at 4°C for 2 h. 500 μg of protein lysate was incubated
276 with the beads for 2 h at 4°C. Beads were washed 3 times with 1x Buffer A, 0.1% Triton-
277 X and eluted with 50 μL of 2x Laemmli buffer.

278 Streptavidin pulldown was largely as described[8], with minor modifications. Cell lysates
279 were diluted to 4 mg/mL before a 2 h incubation with beads. For co-precipitation
280 experiments, separate cells were transfected with each DNA construct, and pre-
281 specified amounts of lysates were combined with each other or with untransfected
282 lysate, such that the total amount of lysate were similar in each experimental condition;
283 these lysates were then incubated at 37°C overnight. To reduce non-specific binding,
284 lysates were pre-cleared with streptavidin beads and then were incubated for 2 h at
285 30°C with 4 μg biotinylated *E. coli* O111:B4 LPS loaded onto 8 μg of Streptavidin Mag
286 sepharose (GE, 28985738, or Pierce, 88816).

287 **Plate binding assays.** Clear flat bottom Nunc Maxisorp ELISA plates (Thermo Fisher,
288 442404) were coated with various concentrations of purified recombinant caspase-4
289 (Origene, TP760359) overnight at 4°C. The plates were washed 3x with PBS then
290 blocked for 2 h at RT with 1% bovine serum albumin (Fisher, BP9700100) in PBS.
291 Excess blocking solution was removed. HEK 293T cells transiently expressing FLAG-
292 NLRP11 and control untransfected cells were lysed into 50 mM Tris-HCl pH 7.4, 150

293 mM NaCl, 5 mM $MgCl_2$, 100 µg/ml digitonin (Thermo Fisher Scientific, BN2006) and
294 complete Mini EDTA-free protease inhibitor (Roche), as described[32]. Total protein
295 concentration of lysates was normalized to 2 mg/mL. Serial dilutions were in
296 untransfected HEK293T cell lysate. Varying concentrations of cell lysates were
297 incubated with pre-blocked ELISA plates for 1 h at RT. Excess lysate was removed by
298 washing 3 times with PBS. For detection of FLAG-NLRP11, wells were incubated with
299 0.8 µg/mL anti-FLAG rabbit (Sigma, F7425-.2MG) was incubated for 1 h at RT, and
300 after washing with PBS, 0.16 µg/mL goat-anti-rabbit conjugated to horseradish
301 peroxidase (HRP) (Jackson, 111-035-144). To detect caspase-4 bound to the plate,
302 wells were incubated with 0.5 µg/mL anti-caspase-4 (Santa Cruz, sc-56056) and, after
303 washing with PBS, 0.16 µg/mL goat-anti-mouse conjugated to HRP (Jackson, 115-035-
304 003), each for 1 hr. After 6 washes with PBS, 50 µL of One Step Ultra-TMB (Fisher
305 Scientific, PI34029) was added to each well and incubated for 5 min before stopping
306 with 4 N sulfuric acid and reading in a BioTek plate reader.

307 **Bacterial infection.** Overnight cultures were started from a single colony taken from a
308 freshly streaked plate. Infections with *S. flexneri* were performed with exponential phase
309 bacteria, after back-dilution from overnight cultures. Infections with *L. monocytogenes*
310 were performed with stationary phase bacteria from overnight cultures. Infections were
311 with a multiplicity of infection (MOI) of 10 for *S. flexneri* cultures and 1 for *L.*
312 *monocytogenes*. Bacteria were centrifuged onto cells at 2000 rpm for 10 min, followed
313 by incubation at 37°C. After 30 min, the cells were washed twice, and then 25 µg/mL
314 gentamicin was added to the media to kill extracellular bacteria. Where appropriate *S.*

315 *enterica* serovar Minnesota LPS was added to 10 μg/mL at the time of infection and
316 MCC950 to 1 μM 30 min prior to infection and maintained during infection. For LDH
317 assays of *S. flexneri* infected cells, 100 μL of cell culture supernatant was collected at 2
318 h and 30 min and at 5 h and/or 30 min of infection; for detection of caspases and/or
319 gasdermin D by western blot, 100 μL of cell culture supernatant was collected at the
320 same time points and was mixed with 35 μL 4x Laemmli buffer supplemented with
321 cOmplete EDTA-free protease inhibitors (Roche, 5056489001). For parallel analyses of
322 *L. monocytogenes* infected cells, gentamicin was used at 15 μg/mL, and samples were
323 collected at 6 h of infection. For western blot analyses, whole cell lysates were collected
324 in 2x Laemmli buffer.

325 Infections with *B. thailandensis* and *S.* Typhimurium were performed with exponential
326 phase bacteria at a multiplicity of infection (MOI) of 10. Bacteria were centrifuged onto
327 cells at 2000 rpm for 10 min, followed by incubation at 37°C. For *S.* Typhimurium, after
328 30 min incubation, the cells were washed twice, and then 25 μg/mL gentamicin was
329 added to the media to kill extracellular bacteria. For *B. thailandensis*, after 2 h
330 incubation, the cells were washed twice with cRPMI. For LDH assays with *S.*
331 Typhimurium infection, 100 μL of cell culture supernatant was collected at 2 h and 30
332 min and at 5 h and 30 min of infection and, for LDH assays with *B. thailandensis*, 100
333 μL of cell culture supernatant was collected at 24 h.

334 **Isolation of primary human peripheral blood mononuclear cells (PBMCs) and**
335 **CD14 monocytes.** Cells were isolated from leukopaks from individual healthy donors
336 (Crimson Core Laboratories, Brigham and Women's Hospital) using density-gradient

337 centrifugation. Briefly, blood was diluted 1:2 with RPMI-1640 (Gibco), layered on top of
338 Ficoll-Paque Plus (GE Healthcare) using SepMate™-50 (IVD) (StemCell Technologies),
339 and centrifuged at 1,200g for 20 min. The PBMC layer was collected and resuspended
340 in 50 ml RPMI-1640 (Gibco) and centrifuged again at 300 g for 10 min. The cells were
341 counted, resuspended in Cryostor CS10 (StemCell Technologies), and aliquoted in
342 cryopreservation tubes at a concentration of 1×10^8 cells per mL. The tubes were
343 placed at −80°C overnight, then transferred to liquid nitrogen for long-term storage. To
344 isolate CD14+ cells, EasySep™ Human CD14 Positive Selection Kit II (StemCell
345 Technologies) was used, following the manufacturer's instructions. Cells were cultured
346 in complete RPMI, differentiated with 25 ng/mL m-CSF (StemCell Technologies), and
347 maintained at 37°C in 5% CO_2.

348 **LPS transfection.** Electroporation of cells with LPS was performed using the Neon
349 Transfection System (Invitrogen) according to the manufacturer's instructions using *S.*
350 Minnesota LPS at indicated concentrations. THP-1 cells were seeded in low-attachment
351 10 cm dishes with 50 ng/mL PMA in RPMI. After 48 h, the cells were lifted in PBS
352 (without calcium or magnesium). For electroporation, 1.5×10^6 THP-1 cells were
353 pelleted, resuspended in Resuspension Buffer R with 2 μg/mL of LPS or water control.
354 Using a 10 μL Neon tip, cells were pulsed once at 1400 V and 10 ms pulse width. For
355 primary human macrophage cells, 7.5×10^5 CD14 macrophages were pelleted, then
356 resuspended in Resuspension Buffer T with 2 μg/mL of LPS or water control. Using a
357 10 μL Neon tip, cells were pulsed 2 times at 2250 V and 20 ms pulse width.
358 Electroporated cells were immediately resuspended in 2 mL of RPMI and placed into

359 wells of a 24 well plate. Cells were incubated for 2.5 h at 37°C before measuring LDH
360 release.

361 **siRNA transient knockdowns.** siRNAs used for NLRP11 knockdowns were
362 Hs_NALP11_1 FlexiTube siRNA and Hs_NALP11_5 FlexiTube siRNA at 10 nM total (5
363 nM each siRNA); for caspase-4 knockdowns were 3941, 4036 and 4130 at 30 nM total
364 (10 nM each siRNA) (ThermoFisher); for Caspase-1 Hs_CASP1_14 FlexiTube siRNA
365 and Hs_CASP1_13 FlexiTube siRNA at 30 nM total (15 nM each siRNA); and for
366 MyD88 Hs_MYD88_5 FlexiTube siRNA and Hs_MYD88_11 FlexiTube siRNA at 30 nM
367 total (15 nM each siRNA) (Qiagen). AllStars Negative Control siRNAs (Qiagen) were
368 used as negative controls at 10 nM or 30 nM, accordingly. siRNAs were transfected
369 using the HiPerfect reagent (Qiagen) into primary human monocyte-derived
370 macrophages 72 h before or into THP-1 cells 48 h before experimental assays,
371 following the manufacturer's protocol for "Transfection of Differentiated Macrophage
372 Cell Lines." After transfection, cells were maintained at 37°C in 5% CO_2. Degree of
373 knock-down was assessed by western blot of lysates of equivalent numbers of cells for
374 each condition.

375 **Nigericin.** PMA differentiated THP-1 cells were washed once with fresh RPMI and
376 primed with 1 μM O55:B5 *E. coli* LPS for 3 h, at which time 10 μM nigericin or vehicle
377 control was added. LDH release was assayed at indicated times after treatment.

378 **LDH assay.** LDH was measured using an LDH Cytotoxicity Kit (Pierce, 88953) or
379 Cytotoxicity Detection Kit (Sigma, 11644793001) per the manufacturer's instructions.
380 Measurements at 490 nm and 680 nm were taken immediately after addition of Stop

381 Solution using a BioTek Plate Reader. To determine LDH activity, the 680 nm
382 absorbance value (background) was subtracted from the 490-nm absorbance value,
383 and cytotoxicity was calculated for each sample as LDH activity as a fraction of the total
384 LDH activity for cells treated with the Triton X-100 lysis buffer provided by the
385 manufacturer. For experiments involving primary cells, a different donor was used for
386 each biological replicate; due to inherent variability from donor to donor in the baseline
387 levels of death in cell death assays, within-donor data were normalized to the negative
388 control condition before compilation of the biological replicates.

389 **Statistics and reproducibility.** Unless otherwise indicated, all results are data from at
390 least 3 independent biological replicates. On bar graphs, each individual symbol is data
391 from an independent biological replicate. Statistical analysis was performed with Prism
392 version 9.

393 **Data availability.** All relevant data are included in the manuscript and will be made
394 available by request to the corresponding author, marcia.goldberg@mgh.harvard.edu.

395 **Supplementary information**

396 The online version contains supplementary material.

397 **Acknowledgements**

398 We thank Jonathan Kagan, Hao Wu, Kate Fitzgerald, Sunny Shin, Ann Goldfeld,
399 Margaret Kielian, Peggy Cotter, and Jeffrey Miller for reagents.

400 This work was supported by a Real Colegio Complutense Fellowship from the Real
401 Colegio Complutense at Harvard (to M.L.G.M.) and NIH grants R01 AI081724 (to
402 M.B.G), F32 AI145128 (to A.S.Z.), F32 AI126765 (to K.A.M.), and T32 AI007061 (to
403 A.S.Z.). The findings and conclusions are solely the responsibility of the authors and to
404 not necessarily represent the official views of NIAID or NIH.

405 **Author contributions**

406 M.B.G. conceived the study, supervised the project, and wrote the manuscript with input
407 from all authors; M.R.L. K.A.M., A.C.H., V.K., and K.T.E. performed cell-based
408 experiments; A.S.Z., T.E.W., and M.L.G.M. performed biochemical experiments. All
409 authors organized and analyzed data and edited the manuscript.

410 **Competing interests**

411 The authors declare no competing interests.

412 **Materials and correspondence**

413 Correspondence and material requests should be addressed to M.B.G.

References

1 Broz, P. & Dixit, V. M. Inflammasomes: mechanism of assembly, regulation and signalling. *Nat Rev Immunol* **16**, 407-420, doi:10.1038/nri.2016.58 (2016).

2 Jorgensen, I., Rayamajhi, M. & Miao, E. A. Programmed cell death as a defence against infection. *Nat Rev Immunol* **17**, 151-164, doi:10.1038/nri.2016.147 (2017).

3 Brewer, S. M., Brubaker, S. W. & Monack, D. M. Host inflammasome defense mechanisms and bacterial pathogen evasion strategies. *Curr Opin Immunol* **60**, 63-70, doi:10.1016/j.coi.2019.05.001 (2019).

4 Wright, S. S., Vasudevan, S. O. & Rathinam, V. A. Mechanisms and Consequences of Noncanonical Inflammasome-Mediated Pyroptosis. *J Mol Biol*, 167245, doi:10.1016/j.jmb.2021.167245 (2021).

5 Kayagaki, N. *et al.* Non-canonical inflammasome activation targets caspase-11. *Nature* **479**, 117-121, doi:10.1038/nature10558 (2011).

6 Kayagaki, N. *et al.* Noncanonical inflammasome activation by intracellular LPS independent of TLR4. *Science* **341**, 1246-1249, doi:10.1126/science.1240248 (2013).

7 Hagar, J. A., Powell, D. A., Aachoui, Y., Ernst, R. K. & Miao, E. A. Cytoplasmic LPS activates caspase-11: implications in TLR4-independent endotoxic shock. *Science* **341**, 1250-1253, doi:10.1126/science.1240988 (2013).

8 Shi, J. *et al.* Inflammatory caspases are innate immune receptors for intracellular LPS. *Nature* **514**, 187-192, doi:10.1038/nature13683 (2014).

9 Kayagaki, N. *et al.* Caspase-11 cleaves gasdermin D for non-canonical inflammasome signalling. *Nature* **526**, 666-671, doi:10.1038/nature15541 (2015).

10 Shi, J. *et al.* Cleavage of GSDMD by inflammatory caspases determines pyroptotic cell death. *Nature* **526**, 660-665, doi:10.1038/nature15514 (2015).

11 Ding, J. *et al.* Pore-forming activity and structural autoinhibition of the gasdermin family. *Nature* **535**, 111-116, doi:10.1038/nature18590 (2016).

12 He, W. T. *et al.* Gasdermin D is an executor of pyroptosis and required for interleukin-1beta secretion. *Cell Res* **25**, 1285-1298, doi:10.1038/cr.2015.139 (2015).

13 Schmid-Burgk, J. L. *et al.* Caspase-4 mediates non-canonical activation of the NLRP3 inflammasome in human myeloid cells. *Eur J Immunol* **45**, 2911-2917, doi:10.1002/eji.201545523 (2015).

14 Baker, P. J. *et al.* NLRP3 inflammasome activation downstream of cytoplasmic LPS recognition by both caspase-4 and caspase-5. *Eur J Immunol* **45**, 2918-2926, doi:10.1002/eji.201545655 (2015).

15 Liu, X. *et al.* Inflammasome-activated gasdermin D causes pyroptosis by forming membrane pores. *Nature* **535**, 153-158, doi:10.1038/nature18629 (2016).

16 Russo, B. C. *et al.* Intermediate filaments enable pathogen docking to trigger type 3 effector translocation. *Nat Microbiol* **1**, 16025, doi:10.1038/nmicrobiol.2016.25 (2016).

17 Watson, J. L. *et al.* Shigella sonnei O-Antigen Inhibits Internalization, Vacuole Escape, and Inflammasome Activation. *mBio* **10**, doi:10.1128/mBio.02654-19 (2019).

18 Zychlinsky, A., Prevost, M. C. & Sansonetti, P. J. Shigella flexneri induces apoptosis in infected macrophages. *Nature* **358**, 167-169, doi:10.1038/358167a0 (1992).
19 Suzuki, T. *et al.* Differential regulation of caspase-1 activation, pyroptosis, and autophagy via Ipaf and ASC in Shigella-infected macrophages. *PLoS Pathog* **3**, e111, doi:10.1371/journal.ppat.0030111 (2007).
20 Ellwanger, K. *et al.* The NLR family pyrin domain-containing 11 protein contributes to the regulation of inflammatory signaling. *The Journal of biological chemistry* **293**, 2701-2710, doi:10.1074/jbc.RA117.000152 (2018).
21 Wu, C. *et al.* NLRP11 attenuates Toll-like receptor signalling by targeting TRAF6 for degradation via the ubiquitin ligase RNF19A. *Nat Commun* **8**, 1977, doi:10.1038/s41467-017-02073-3 (2017).
22 Qin, Y. *et al.* NLRP11 disrupts MAVS signalosome to inhibit type I interferon signaling and virus-induced apoptosis. *EMBO Rep* **18**, 2160-2171, doi:10.15252/embr.201744480 (2017).
23 Sanada, T. *et al.* The Shigella flexneri effector OspI deamidates UBC13 to dampen the inflammatory response. *Nature* **483**, 623-626, doi:10.1038/nature10894 (2012).
24 Gaillard, J. L., Berche, P., Mounier, J., Richard, S. & Sansonetti, P. In vitro model of penetration and intracellular growth of Listeria monocytogenes in the human enterocyte-like cell line Caco-2. *Infect Immun* **55**, 2822-2829 (1987).
25 Meunier, E. *et al.* Caspase-11 activation requires lysis of pathogen-containing vacuoles by IFN-induced GTPases. *Nature* **509**, 366-370, doi:10.1038/nature13157 (2014).
26 Beuzon, C. R. *et al.* Salmonella maintains the integrity of its intracellular vacuole through the action of SifA. *The EMBO journal* **19**, 3235-3249, doi:10.1093/emboj/19.13.3235 (2000).
27 Grenier, J. M. *et al.* Functional screening of five PYPAF family members identifies PYPAF5 as a novel regulator of NF-kappaB and caspase-1. *FEBS letters* **530**, 73-78, doi:10.1016/s0014-5793(02)03416-6 (2002).
28 Bitto, N. J. *et al.* Membrane vesicles from Pseudomonas aeruginosa activate the noncanonical inflammasome through caspase-5 in human monocytes. *Immunol Cell Biol* **96**, 1120-1130, doi:10.1111/imcb.12190 (2018).
29 Pilla, D. M. *et al.* Guanylate binding proteins promote caspase-11-dependent pyroptosis in response to cytoplasmic LPS. *Proc Natl Acad Sci U S A* **111**, 6046-6051, doi:10.1073/pnas.1321700111 (2014).
30 Fisch, D. *et al.* Human GBP1 is a microbe-specific gatekeeper of macrophage apoptosis and pyroptosis. *The EMBO journal* **38**, e100926, doi:10.15252/embj.2018100926 (2019).
31 Santos, J. C. *et al.* LPS targets host guanylate-binding proteins to the bacterial outer membrane for non-canonical inflammasome activation. *The EMBO journal* **37**, doi:10.15252/embj.201798089 (2018).
32 Wandel, M. P. *et al.* Guanylate-binding proteins convert cytosolic bacteria into caspase-4 signaling platforms. *Nat Immunol* **21**, 880-891, doi:10.1038/s41590-020-0697-2 (2020).

33 Santos, J. C. *et al.* Human GBP1 binds LPS to initiate assembly of a caspase-4 activating platform on cytosolic bacteria. *Nat Commun* **11**, 3276, doi:10.1038/s41467-020-16889-z (2020).
34 Kim, B. H., Shenoy, A. R., Kumar, P., Bradfield, C. J. & MacMicking, J. D. IFN-inducible GTPases in host cell defense. *Cell host & microbe* **12**, 432-444, doi:10.1016/j.chom.2012.09.007 (2012).
35 Kutsch, M. *et al.* Direct binding of polymeric GBP1 to LPS disrupts bacterial cell envelope functions. *The EMBO journal* **39**, e104926, doi:10.15252/embj.2020104926 (2020).
36 Paz, I. *et al.* Galectin-3, a marker for vacuole lysis by invasive pathogens. *Cell Microbiol* **12**, 530-544, doi:10.1111/j.1462-5822.2009.01415.x (2010).
37 Feeley, E. M. *et al.* Galectin-3 directs antimicrobial guanylate binding proteins to vacuoles furnished with bacterial secretion systems. *Proc Natl Acad Sci U S A* **114**, E1698-E1706, doi:10.1073/pnas.1615771114 (2017).
38 Lo, T. H. *et al.* Galectin-3 promotes noncanonical inflammasome activation through intracellular binding to lipopolysaccharide glycans. *Proc Natl Acad Sci U S A* **118**, doi:10.1073/pnas.2026246118 (2021).
39 Taveira da Silva, A. M. *et al.* Brief report: shock and multiple-organ dysfunction after self-administration of Salmonella endotoxin. *N Engl J Med* **328**, 1457-1460, doi:10.1056/NEJM199305203282005 (1993).
40 Schaedler, R. W. & Dubos, R. J. The susceptibility of mice to bacterial endotoxins. *J Exp Med* **113**, 559-570 (1961).
41 Labrec, E. H., Schneider, H., Magnani, T. J. & Formal, S. B. Epithelial Cell Penetration as an Essential Step in the Pathogenesis of Bacillary Dysentery. *J Bacteriol* **88**, 1503-1518, doi:10.1128/jb.88.5.1503-1518.1964 (1964).
42 Wing, H. J., Yan, A. W., Goldman, S. R. & Goldberg, M. B. Regulation of IcsP, the outer membrane protease of the Shigella actin tail assembly protein IcsA, by virulence plasmid regulators VirF and VirB. *J Bacteriol* **186**, 699-705, doi:10.1128/JB.186.3.699-705.2004 (2004).
43 Maurelli, A. T., Blackmon, B. & Curtiss, R., 3rd. Loss of pigmentation in Shigella flexneri 2a is correlated with loss of virulence and virulence-associated plasmid. *Infect Immun* **43**, 397-401, doi:10.1128/iai.43.1.397-401.1984 (1984).
44 Miller, K. A., Garza-Mayers, A. C., Leung, Y. & Goldberg, M. B. Identification of interactions among host and bacterial proteins and evaluation of their role early during Shigella flexneri infection. *Microbiology (Reading)* **164**, 540-550, doi:10.1099/mic.0.000637 (2018).
45 Novem, V. *et al.* Structural and biological diversity of lipopolysaccharides from Burkholderia pseudomallei and Burkholderia thailandensis. *Clin Vaccine Immunol* **16**, 1420-1428, doi:10.1128/CVI.00472-08 (2009).
46 Gedde, M. M., Higgins, D. E., Tilney, L. G. & Portnoy, D. A. Role of listeriolysin O in cell-to-cell spread of Listeria monocytogenes. *Infect Immun* **68**, 999-1003, doi:10.1128/IAI.68.2.999-1003.2000 (2000).
47 Datsenko, K. A. & Wanner, B. L. One-step inactivation of chromosomal genes in Escherichia coli K-12 using PCR products. *Proc Natl Acad Sci U S A* **97**, 6640-6645, doi:10.1073/pnas.120163297 (2000).

549 48 Ranjbar, S., Jasenosky, L. D., Chow, N. & Goldfeld, A. E. Regulation of
550 Mycobacterium tuberculosis-dependent HIV-1 transcription reveals a new role for
551 NFAT5 in the toll-like receptor pathway. *PLoS Pathog* **8**, e1002620,
552 doi:10.1371/journal.ppat.1002620 (2012).
553 49 Kobayashi, T. *et al.* The Shigella OspC3 effector inhibits caspase-4, antagonizes
554 inflammatory cell death, and promotes epithelial infection. *Cell host & microbe*
555 **13**, 570-583, doi:10.1016/j.chom.2013.04.012 (2013).
556 50 Li, Z. *et al.* Shigella evades pyroptosis by arginine ADP-riboxanation of caspase-
557 11. *Nature* **599**, 290-295, doi:10.1038/s41586-021-04020-1 (2021).

558

559 **Figures and figure legends**

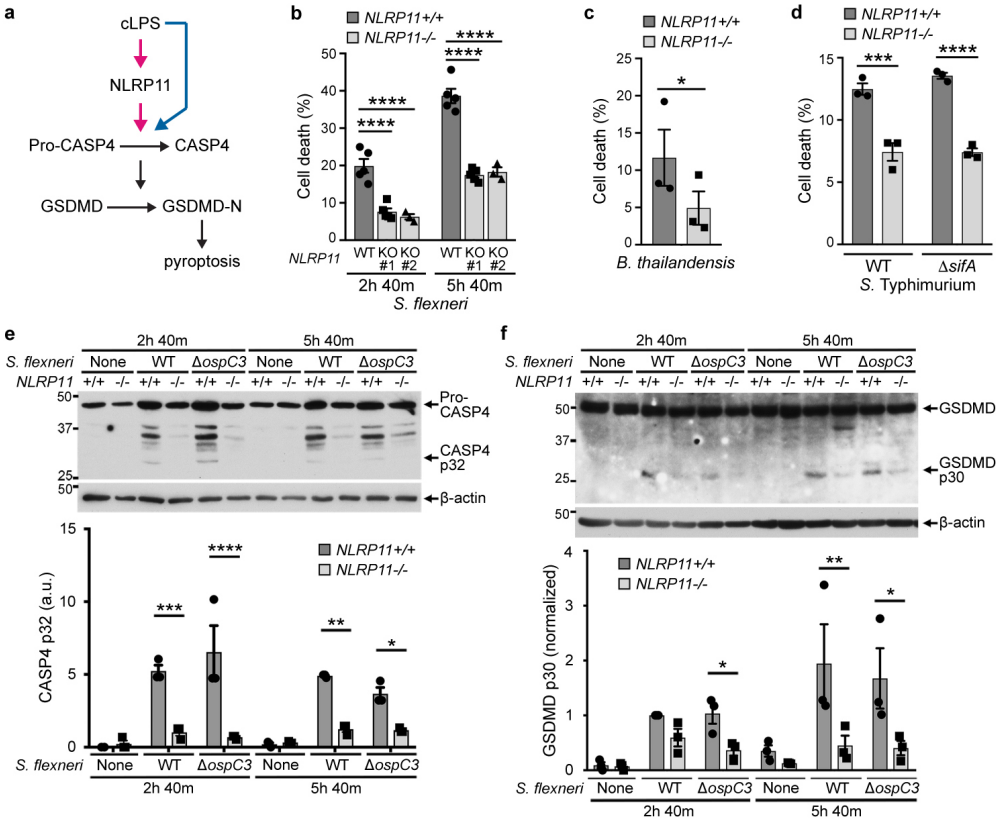

560

561 **Fig. 1. In the absence of *NLRP11*, cell death of human-derived macrophage-like**

562 **cells induced by intracellular gram-negative bacteria is defective.**

563 (**a**) Current (blue/black arrows) and proposed (pink/black arrows) paradigms of non-

564 canonical recognition of cLPS; with high cLPS concentration, both pathways are

565 proposed to occur. CASP4, caspase-4; GSDMD, gasdermin D; GSDMD-N, processed

566 N-terminal domain of GSDMD. (**b**-**c**) Death of THP-1 macrophages upon infection with

567 the cytosolic gram-negative pathogens *S. flexneri* (**b**), and *B. thailandensis* (**c**). Cell

568 death in response to *S. flexneri* infection in each of two independent *NLRP11*$^{-/-}$ THP-1

569 cell lines (**b**). *n* = 5 (**b**: WT, KO #1) or 3 experiments (**b**: KO #2, **c**). (**d**) *NLRP11*

570 dependence of efficient THP-1 macrophage death induced by *S.* Typhimurium. *sifA*

571 mutant, which is largely cytosolic, and WT *S.* Typhimurium, which is largely vacuolar. *n*
572 = 3 experiments. (**e-f**) *NLRP11* dependence of efficient caspase-4 (**e**) and gasdermin D
573 (**f**) processing during *S. flexneri* infection of THP-1 macrophages; western blot of culture
574 supernatants. In the absence of OspC3, processing was similar to induced by WT *S.*
575 *flexneri*; in mouse bone marrow-derived macrophages and human epithelial cell lines,
576 OspC3 arginine ADP riboxanates caspase-4, thereby inhibiting processing of gasdermin
577 D[49,50]. *n* = 3 experiments. Cell death is by LDH release, reported as percent of total
578 Triton X-100 cell lysis. Mean ± S.E.M. Two-way ANOVA with Dunnett *post hoc* test (**b**,
579 **d**) or with Sidak *post hoc* test (**e-f**), or student T-test (**c**). *, $p<0.05$; **, $p<0.01$; ***;
580 $p<0.001$; ****, $p<0.0001$; a.u., arbitrary units.

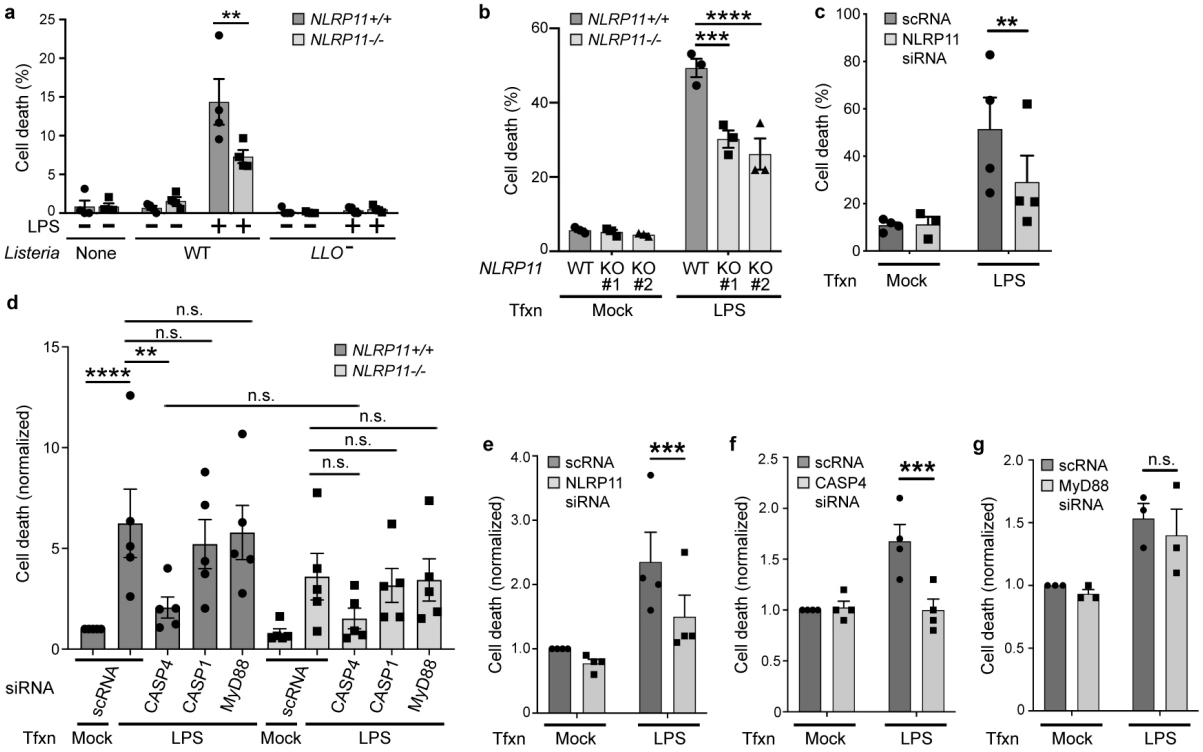

581

582 **Fig. 2. *NLRP11* potentiates cell death in human macrophages in response to**

583 **cytosolic LPS.**

584 (**a**) *NLRP11* potentiates death of THP-1 macrophage-like cells induced by infection with

585 cytosolic gram-positive pathogen *L. monocytogenes* that is coated with *S. enterica*

586 serovar Minnesota LPS. Cell death depends on coating of *L. monocytogenes* with LPS

587 and on escape from the vacuole, as *L. monocytogenes LLO*$^-$ is restricted to the

588 phagosome. *n* = 4 experiments. (**b-c**) In the absence of *NLRP11* (**b**) or following

589 NLRP11 siRNA (**c**), death of THP-1 macrophage-like cells in response to electroporated

590 LPS is defective. *n* = 3 (**b**) or 4 (**c**) experiments. (**d**) NLRP11-dependent cell death of

591 THP-1 macrophage-like cells depends on caspase-4, but not caspase-1 or MyD88. Cell

592 death following siRNA depletion of *CASP4*, *CASP1*, or *MyD88*. *n* = 5 experiments. (**e-g**)

593 NLRP11 is required for efficient cell death of primary human monocyte-derived

594 macrophages in response to cLPS. Cell death in isolated CD14+ cells differentiated to
595 macrophages, treated with siRNA to *NLRP11* (**e**), *caspase-4* (**f**), or *MyD88* (**g**), and
596 subsequently electroporated with LPS. Each experiment performed with cells from a
597 different donor. Cell death measured as LDH release relative to complete lysis control;
598 (**e-g**), normalized to mock transfection following scRNA treatment. *n* = 4 (**e-f**) or 3 (**g**)
599 experiments. Tfxn, transfection; mock, carrier alone; scRNA, scrambled siRNA; CASP4,
600 caspase-4, CASP1, caspase-1. Two-way ANOVA with Sidak *post hoc* test (**a**) or Tukey
601 *post hoc* test (**b-d**); mixed-effects analyses (**e-g**). Mean ± S.E.M. **, p<0.01; ***;
602 p<0.001; ****, p<0.0001; n.s., not significant.

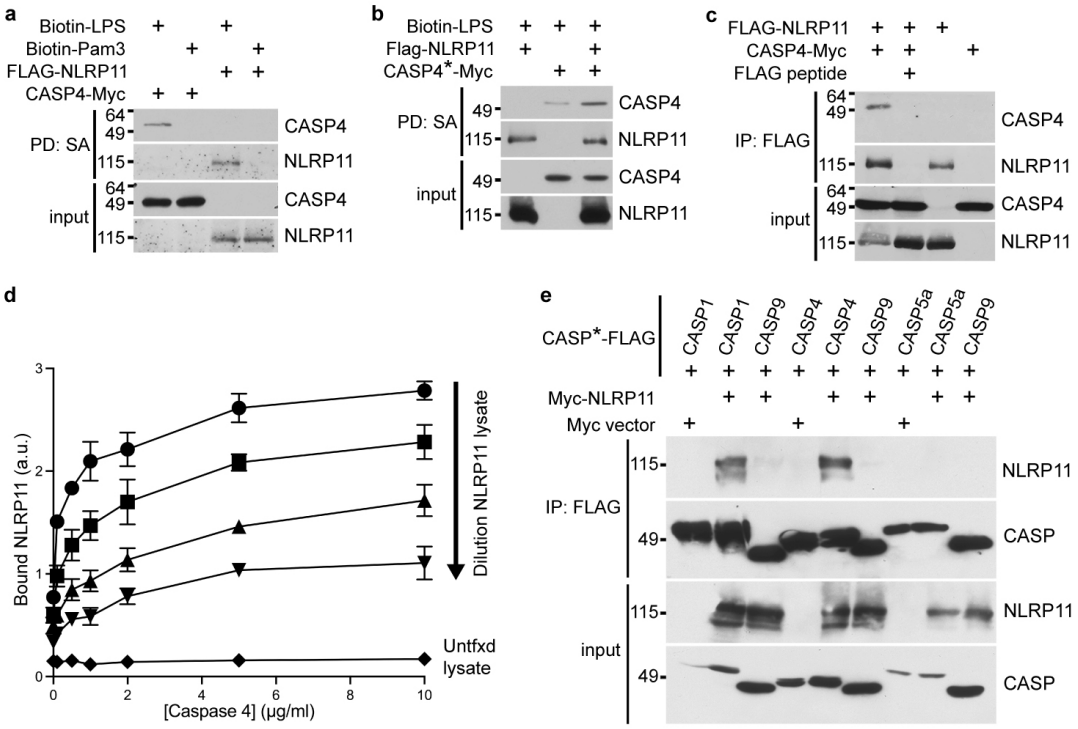

603

604 **Fig. 3. NLRP11 interactions with caspases in reconstituted HEK293T lysates.**

605 (**a-b**) Precipitation of NLRP11 and wildtype caspase-4 (CASP4) by biotin-LPS,
606 separately (**a**) and together (**b**), and not by biotin-PAM3CSK4 (Pam3) (**a**). PD: SA, pull
607 down with streptavidin beads. *n* = 3 experiments. (**c**) NLRP11 precipitates wildtype
608 CASP4. *n* = 3 experiments (**d**) Interaction between NLRP11 and CASP4 increases as a
609 function of the concentration of each protein. Binding of FLAG-NLRP11 in transfected
610 HEK293T cells to plates coated with purified wildtype CASP4 with detection of bound
611 FLAG. Dilutions of NLRP11 lysates: circles, undiluted; squares, 1:2 dilution; triangles,
612 1:4 dilution; inverted triangles, 1:8 dilution. Diamonds, untransfected (untfxd) lysate. *n* =
613 3 experiments. Two-way ANOVA with Tukey *post hoc* test. a.u., arbitrary units. (**e**)
614 Specificity of NLRP11 for caspase-4 and caspase-1. FLAG-tagged catalytically inactive

615 caspases (CASP1[C285A]-FLAG, CASP5a[C315A]-FLAG, CASP9[C287S]-FLAG)

616 precipitation of Myc-NLRP11. CASP*, catalytically inactive caspase. IP: FLAG, pull

617 down with beads coated with FLAG antibody. Detection by western blot with anti-FLAG

618 or anti-Myc antibody. *n* = 3 experiments.